

A Minimal Supersymmetric Kink Model: Exact Solution

Azadeh Mohammadi^a André Amado^b

^a*Departamento de Física, Universidade Federal da Paraíba,
58.059-970, Caixa Postal 5.008, João Pessoa, PB, Brazil*

^b*Departamento de Física, Universidade Federal de Pernambuco,
52171-900 Recife, PE, Brazil*

E-mail: a.mohammadi@fisica.ufpb.br, andreamado@df.ufpe.br

ABSTRACT: In this paper we investigate a minimal supersymmetric soliton model, $\mathcal{N} = 1$, in $(1+1)$ dimensions in which the bosonic part of the potential is the one in $\lambda\phi^4$ theory. In this system a fermion is coupled to a pseudoscalar field nonlinearly. As the set of coupled equations of motion in the system is not analytically solvable without considering the weak coupling approximation, we use a numerical method to solve the system dynamically and nonperturbatively. We obtain the bound energy spectrum, bound states of the system and the corresponding shape of the soliton using a relaxation method except for the zero mode fermionic state and threshold energies that are possible to solve analytically. The results we obtain are consistent with the ones based on the weak coupling approximation which is valid when the coupling goes to zero. With the aid of these results we are able to investigate the strong coupling limit besides the weak coupling one and show how much the soliton is affected in strong and weak coupling regions.

Contents

1	Introduction	1
2	Supersymmetric kink model	2
3	Bound states and bound energies	4
3.1	Zero energy bound state	4
3.2	Threshold states	5
3.3	Numerical Method	5
4	Conclusion	8

1 Introduction

Solitons named by Zabusky and Kruskal in 1965 [1], first appeared as a solution for KdV equation [2]. They play important roles in diverse areas of physics, biology and engineering [3–5]. In one spatial dimension kinks, and in higher spatial dimensions vortices, instantons, monopoles and domain walls, are amongst the important ones in this category. They are topological configurations which appear in different areas of physics such as high energy physics, atomic and condensed matter physics [6–10]. These topologically nontrivial configurations cannot be deformed continuously into a trivial vacuum configuration.

Models including coupled fermionic and bosonic fields are crucial in many branches of physics, specially when the bosonic field has the form of a soliton. As solitons can be viewed as extended particles with finite mass, finite energy at rest, the systems consisting of coupled fermionic and solitonic fields can be a good candidate to describe extended objects such as hadrons. Since 1958, with Skyrme’s pioneering works [11–15], many physicists have tried to explain the hadrons and their strong interactions nonperturbatively using phenomenological nonlinear field theories [16–18].

When a fermion interacts with a soliton, an interesting phenomenon occurs which is the assignment of fractional fermion number to the solitonic state. In a theory where all the fields carry integer quantum numbers, the emergence of fractional quantum numbers has attracted a lot of interest. Much of the work in this area has been inspired by the Jackiw and Rebbi’s pioneering work [19]. The presence of a soliton distorts the vacuum and consequently can induce nonzero vacuum polarization and Casimir energy. Imposing a boundary condition or a background field like soliton can alter the fermionic spectrum in the system which results in Casimir energy. These phenomena have been widely discussed in the literature for different models and different dimensions [20–23].

The issue of quantum corrections to the soliton mass in $(1 + 1)$ dimensional theories, specially in the context of minimal supersymmetric solitons, $\mathcal{N} = 1$, have received a great deal of attention since 1970’s [24, 25]. Supersymmetric soliton models are amongst the most important coupled fermion-soliton systems. BPS saturation in $\mathcal{N} = 1$ supersymmetric solitons at quantum level has a long and controversial history [26–29]. BPS solitons can emerge in the supersymmetric models in which superalgebras are centrally extended, having mass equal to the central charge. Centrally extended supersymmetric algebras admit a special class of massive representations which preserve some fraction of the supersymmetry of the vacuum and consequently form multiplets, shortened or BPS supermultiplets, which are smaller than a generic massive representations. In

supersymmetric theories with solitons, topological quantum numbers appear as central extensions of the supersymmetric algebra. Furthermore, in a certain class of $\mathcal{N} = 2$ supersymmetric field theories some nonperturbative effects have been calculated using dualities between field theories with pointlike particles and field theories with solitons [30, 31].

In most of the models investigated in the literature consisting of coupled fermion-soliton systems, the soliton is considered as a background field. The main reason is that solving the nonlinear system treating both fields as dynamical is in general extremely difficult to do analytically. In principle, the soliton in these systems can have infinitely different shapes. Based on Jackiw and Rebbi's work [19], the back-reaction of the fermion on soliton is small in the weak coupling regime and can be treated perturbatively. Therefore, in the weak coupling region considering soliton to be a prescribed field is a good approximation, although out of this region including strong coupling limit it fails considerably. In this paper we solve a minimal supersymmetric kink model, $\mathcal{N} = 1$, dynamically and exactly (nonperturbatively) within our numerical precision.

This paper is organized in four sections: In section 2 we briefly introduce the minimal supersymmetric kink model in $(1 + 1)$ dimensions and the formulation of the problem. In this section we write the lagrangian describing our model, in components, and the resultant equations of motion. In section 3 we obtain the bound states and bound energies of the system. We find the fermionic zero energy bound state and threshold bound energies analytically. To obtain other fermionic bound energies, bound states and the shape of the soliton, we use a numerical method called relaxation method. In the same section we show and compare the results in weak and strong coupling regimes. At the end of the section we show the so-called soliton mass in the intervals including both weak and strong coupling regions. We also obtain the back-reaction of the fermion on the soliton. Based on the result, we compare the back-reaction in weak and strong coupling regions. Finally, section 4 is devoted to summarize and discuss our results.

2 Supersymmetric kink model

We consider the minimal supersymmetry, $\mathcal{N} = 1$, in a two dimensional field theory. Adding a real Grassmann variable θ_α , one can promote the two dimensional space $x^\mu = \{t, x\}$ to superspace, where $\alpha = 1, 2$. The coordinate transformations that add supersymmetry to the Poincaré invariance are

$$\theta_\alpha \rightarrow \theta_\alpha + \epsilon_\alpha, \quad x^\mu \rightarrow x^\mu - i\bar{\theta}\gamma^\mu\epsilon, \quad (2.1)$$

where $\bar{\theta} = \theta\gamma^0$. The superfield $\Phi(x, \theta)$ is a function defined in superspace and has the following form

$$\Phi(x, \theta) = \phi(x) + \bar{\theta}\psi(x) + \frac{1}{2}\bar{\theta}\theta F(x). \quad (2.2)$$

The supersymmetric action is

$$S = i \int d^2\theta d^2x \left\{ \frac{1}{4} \bar{D}_\alpha \Phi D_\alpha \Phi + W(\Phi) \right\}, \quad (2.3)$$

which is invariant under the transformations

$$\delta\phi = \bar{\epsilon}\psi, \quad \delta\psi = -i\partial_\mu\phi\gamma^\mu\epsilon + F\epsilon, \quad \delta F = -i\bar{\epsilon}\gamma^\mu\partial_\mu\psi. \quad (2.4)$$

The spinorial derivatives are defined as

$$D_\alpha = \frac{\partial}{\partial\theta_\alpha} - i(\gamma^\mu\theta)_\alpha\partial_\mu, \quad \bar{D}_\alpha = -\frac{\partial}{\partial\bar{\theta}_\alpha} - i(\bar{\theta}\gamma^\mu)_\alpha\partial_\mu. \quad (2.5)$$

In components, the supersymmetric lagrangian ends up with the form [27]

$$\mathcal{L} = \frac{1}{2} (\partial_\mu \phi \partial^\mu \phi + \bar{\psi} i \gamma^\mu \partial_\mu \psi + F^2) + W_\phi F - \frac{1}{2} W_{\phi\phi} \bar{\psi} \psi, \quad (2.6)$$

where the subscript ϕ shows the derivative with respect to ϕ . Using the Euler-Lagrange equations and choosing the bosonic potential to be the kink potential $V(\phi) = \frac{\lambda}{4} \left(\phi^2 - \frac{m^2}{\lambda} \right)^2$, i.e. $V(\phi) = \frac{1}{2} W_\phi^2$, we obtain

$$\mathcal{L}_{kink} = \frac{1}{2} \partial_x \phi \partial^x \phi + \frac{1}{2} \bar{\psi} i \gamma^\mu \partial_\mu \psi - \sqrt{\frac{\lambda}{2}} \phi \bar{\psi} \psi - \frac{\lambda}{4} \left(\phi^2 - \frac{m^2}{\lambda} \right)^2, \quad (2.7)$$

in which ϕ is considered static.

In order to guarantee a well-defined energy for the soliton, we have $\phi(x \rightarrow \pm\infty) = \pm \frac{m}{\sqrt{\lambda}} \equiv \pm\theta_0$.

It is interesting to notice that the supersymmetry relates the fermionic and bosonic couplings, i.e. the parameter λ , although they can be different in general [19, 32].

The representation for the Dirac matrices is chosen as $\gamma^0 = \sigma_1$, $\gamma^1 = i\sigma_3$ and $\gamma^5 = \sigma_2$. Defining $\chi = \phi/\theta_0$ and $\psi = \begin{pmatrix} \psi_1 + i\psi_3 \\ \psi_2 + i\psi_4 \end{pmatrix}$, the equations of motion for the system are

$$\begin{aligned} E \psi_1 + \psi_2' - \sqrt{2}m \chi \psi_2 &= 0, \\ E \psi_2 - \psi_1' - \sqrt{2}m \chi \psi_1 &= 0, \\ E \psi_3 + \psi_4' - \sqrt{2}m \chi \psi_4 &= 0, \\ E \psi_4 - \psi_3' - \sqrt{2}m \chi \psi_3 &= 0, \\ -\chi'' + m^2 \chi (\chi^2 - 1) + \sqrt{2} \frac{\lambda}{m} (\psi_1 \psi_2 + \psi_3 \psi_4) &= 0, \end{aligned} \quad (2.8)$$

where prime denotes the differentiation with respect to x . Due to the symmetry in the equation system, there are only two independent degrees of freedom in ψ . Therefore, we can solve only the real part of the spinor field. Also, we rescale all the quantities to dimensionless ones as $\psi \rightarrow \sqrt{m} \psi$, $\chi \rightarrow \chi$, $E \rightarrow mE$, $\lambda \rightarrow m^2 \lambda$ and $x \rightarrow x/m^1$.

As can be seen in the lagrangian (2.7), the fermion field interacts nonlinearly with the pseudoscalar field. The system cannot be solved analytically without imposing the soliton to be a background field. Thus, we solve this coupled set of equations dynamically and find the fermionic bound states and bound energies as well as the shape of the soliton using a numerical method. We use dynamical in the sense that this work goes beyond the perturbation theory, where the back-reaction of the fermion on soliton is small in the weak coupling regime and can be calculated perturbatively. The main advantage is to help us understand the system in both strong and weak coupling regimes.

In the weak coupling limit, $\lambda \rightarrow 0$ ($\theta_0 \rightarrow \infty$), the last equation in (2.8) decouples from the others and has analytical solution, i.e. kink of $\lambda \phi^4$ theory. The solutions of some analogous systems in this limit have been studied in detail in [19, 32]. In this limit, the solution for this equation is

$$\chi_{st}(x) = \tanh \left(\frac{x - x_0}{\sqrt{2}} \right), \quad (2.9)$$

and there are five fermionic bound states with energies $0, \pm\sqrt{\frac{3}{2}}(m)$ and $\pm\sqrt{2}(m)$. The $E = \pm\sqrt{2}(m)$ states are threshold states as the bound state goes to a constant at infinity.

¹We write the mass dimension in parenthesis when deemed necessary in order to avoid confusion.

One can calculate the so-called soliton mass using the expression

$$M = \int_{-\infty}^{\infty} \left(\frac{1}{2} (\theta_0 \chi)^{\prime 2} + V(\theta_0 \chi) \right) dx \quad (2.10)$$

that is $M = \frac{2\sqrt{2}}{3} m \theta_0^2$ for the kink of $\lambda \phi^4$ theory. We solve the set of coupled equations (2.8) self-consistently and check the results with the ones in the weak coupling limit.

3 Bound states and bound energies

We obtain zero energy bound state and threshold energies analytically, although to find the other bound states we have to rely on our numerical method.

3.1 Zero energy bound state

For this state the equations of motion are simplified and we are able to obtain the analytical solution of the system in the whole θ_0 interval. Interestingly, the solutions show to be independent of θ_0 .

Imposing $E = 0$, the equation system becomes

$$\begin{aligned} \psi_1' + \sqrt{2} \chi \psi_1 &= 0, \\ \psi_2' - \sqrt{2} \chi \psi_2 &= 0, \\ -\chi'' + \chi (\chi^2 - 1) + \frac{\sqrt{2}}{\theta_0^2} \psi_1 \psi_2 &= 0. \end{aligned} \quad (3.1)$$

It turns out that the first two equations can be easily solved as functions of χ , yielding

$$\begin{aligned} \psi_1(x) &= a_1 e^{\int_1^x -\sqrt{2} \chi(x') dx'}, \\ \psi_2(x) &= a_2 e^{\int_1^x \sqrt{2} \chi(x') dx'}. \end{aligned} \quad (3.2)$$

Noticing that if we define $f(x) \equiv e^{\int_1^x \sqrt{2} \chi(x') dx'}$, either $f(x \rightarrow \pm\infty) = 0$ and $f^{-1}(x \rightarrow \pm\infty)$ diverges or $f^{-1}(x \rightarrow \pm\infty) = 0$ and $f(x \rightarrow \pm\infty)$ diverges. As the normalization of the divergent components should be zero, we can conclude either $a_1 = 0$ or $a_2 = 0$. Thus, the term with ψ dependence in the last equation vanishes and we find

$$-\chi'' + \chi (\chi^2 - 1) = 0, \quad (3.3)$$

which corresponds to the trivial kink equation with the known solution (eq. (2.9)).

This way one can determine $f(x) = e^{\int_1^x \sqrt{2} \tanh[(x'-x_0)/\sqrt{2}] dx'} \propto \cosh^2\left(\frac{x-x_0}{\sqrt{2}}\right)$. Requiring the wave function to be normalized, we obtain

$$\psi(x) = \sqrt{\frac{3}{4\sqrt{2}}} \begin{pmatrix} \cosh^{-2}\left(\frac{x-x_0}{\sqrt{2}}\right) \\ 0 \end{pmatrix}. \quad (3.4)$$

It is important to notice that based on this result, the back-reaction of the fermion on the soliton is zero for the fermionic zero mode. This result would be expected if a system has particle conjugation symmetry. If a system does not possess this symmetry the back-reaction for the fermionic zero mode can be nonzero, in general [33]. Surprisingly, although the system considered here does not respect this symmetry, except in the weak coupling limit, it has the same property which means that this symmetry still has an imprint on the system. This property holds for the lagrangian considered in [19, 32] with different fermionic and bosonic couplings.

3.2 Threshold states

Threshold or half-bound states are the states appearing in 1+1 Quantum Field Theory where the fermion field goes to a constant at spacial infinity. For these states when $x \rightarrow \infty$ the wave function is finite, but does not decay fast enough to be square-integrable [29, 34, 35].

To find such states in our system we solve the system of equations at $x \rightarrow \pm\infty$. We write ψ in the form $\psi(x \rightarrow \pm\infty) = \begin{pmatrix} c_1 \\ c_2 \end{pmatrix}$, where c_i 's are arbitrary constants.

Applying the conditions $\chi(x \rightarrow \pm\infty) = \pm 1$, $\chi'(x \rightarrow \pm\infty) = \chi''(x \rightarrow \pm\infty) = 0$ and $\psi'(x \rightarrow \pm\infty) = \begin{pmatrix} 0 \\ 0 \end{pmatrix}$ to the set of equations of motion, we obtain

$$\begin{aligned} E c_1 - \sqrt{2} \chi c_2 &= 0, \\ E c_2 - \sqrt{2} \chi c_1 &= 0, \\ \frac{\sqrt{2}}{\theta_0^2} c_1 c_2 &= 0. \end{aligned} \tag{3.5}$$

The constants c_1 and c_2 can be either zero or nonzero constants in general when the energy is nonzero. If c_1 and c_2 are nonzero constants, this system has solution only in the weak coupling limit, $\theta_0 \rightarrow \infty$. Solving the system in this limit, it is easy to show that the energy of the threshold states are $E = \pm\sqrt{2}(m)$, as expected.

Except for the limit $\theta_0 \rightarrow 0$, the back-reaction of fermion on soliton is finite. When the disturbance region is finite, the continuum fermionic state should tend to the plane wave out of this region. Therefore, the threshold fermionic state should go to a nonzero constant to match both bound and continuum regions. This condition holds everywhere except for the limit $\theta_0 \rightarrow 0$, as can be seen in the last equation of (2.8). It means that, except for this limit, no bound state arises from or joins continua besides those at the weak coupling limit.

3.3 Numerical Method

The other bound states cannot be found analytically and a numerical method is required. We use a relaxation method that starts with an initial guess and iteratively converges to the solution of the system. We start with the known energy spectrum and bound states in the weak coupling limit [32] and find the solution for the whole region of θ_0 including the strong coupling region.

There are two first order differential equations and one second order equation (eq. (2.8)) that can be transformed to a set of two first order equations as

$$p \equiv \chi', \quad -p' + \chi(\chi^2 - 1) + \frac{\sqrt{2}\lambda}{m} \psi_1 \psi_2 = 0. \tag{3.6}$$

In order to calculate the energy we add one more equation $E' = 0$, reflecting the fact that energy is spatially constant. Moreover, we fix the translational symmetry of the system by choosing $x_0 = 0$.

Now, there are five coupled first-order differential equations to solve which need five boundary conditions. Among the several boundary conditions available, we choose the following

$$\chi(\pm\infty) = \pm 1, \quad \chi(0) = 0, \quad \psi_1(\pm\infty) = 0. \tag{3.7}$$

Left graph in figure 1 shows the fermionic bound state energies as a function of the asymptotic value of the bosonic field, θ_0 . As can be seen, the weak coupling limit result is retrieved as $\theta_0 \rightarrow \infty$, i.e. $E = \pm\sqrt{3}/2$. It is important to note that for $\theta_0 \gtrsim 2$ the dynamical graphs and the lines $E = \pm\sqrt{3}/2$ are not easily distinguishable, although for smaller θ_0 the negative and positive energies change drastically from the ones in the weak coupling limit. In the numerical simulations

the closer θ_0 is to zero, more difficult is for the solutions to converge. Thus, the smallest values of θ_0 we are able to obtain are $\theta_0 = 0.501$ for the positive bound energy and $\theta_0 = 0.564$ for the negative one, though based on physical intuition it is possible to guess partially how the energy curves would behave below these values. The positive bound energy curve should not cross the zero energy line as it would configure level crossing [32]. Furthermore, as the negative energy curve becomes closer to the threshold line $E = -\sqrt{2}$, its slope decreases considerably at $\theta_0 \approx 0.63$, as the right graph of figure 1 shows. It means that it probably does not join the Dirac sea, except for the limit $\theta_0 \rightarrow 0$, which is consistent with the discussion in the section 3.2.

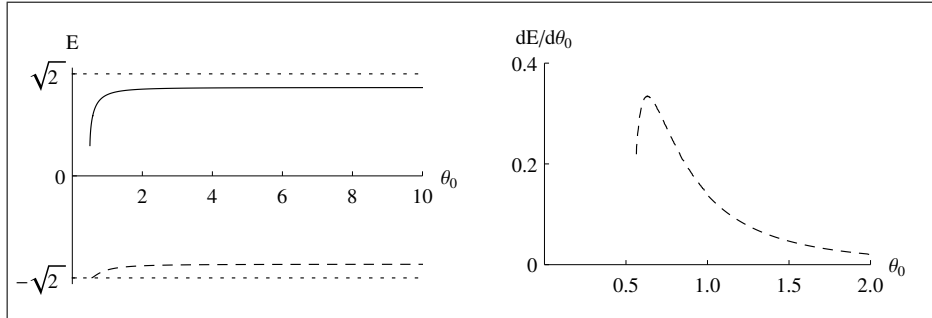


Figure 1. Left graph: The fermionic bound state energies as a function of θ_0 . Solid and dashed curves depict the positive and negative fermionic bound state energies, respectively, in the dynamical model. Dotted lines depict the fermionic threshold energies in the weak coupling limit. Right graph: The derivative of the fermionic negative bound energy with respect to θ_0 as a function of θ_0 .

Figures 2 and 3 depict the fermionic bound states as a function of x for positive and negative energies, respectively. The solid curves are the result of our dynamical model and the dotted ones are the result in the weak coupling limit. We show the results for two different low values of θ_0 for positive and negative energy states in order to highlight the effects in the strong coupling region. As can be seen in the graphs, in lower θ_0 the dynamical and static results become more different which confirms that in the low θ_0 region the system cannot be described by the weak coupling approximation.

To investigate the effect of the fermion on the shape of the soliton, in Figures 4 and 5 we show the bosonic field as a function of x for positive and negative energies, respectively. As before, the solid curves show the result of the dynamical model and the dotted ones the result for model with prescribed soliton. Since the results for positive energy change considerably in low θ_0 region, we show the result for three different values of θ_0 to make it possible to track the transition to the strong coupling limit. For each of the graphs we show χ and its spatial derivative, χ' , to illustrate how the soliton changes from the prescribed one. It is important to notice that although the soliton can change drastically in the strong coupling region, the changes are limited to a small region around the origin. This result confirms that the back-reaction of the fermion on the soliton and thus the disturbance region are finite, except for the limit $\theta_0 \rightarrow 0$, which is also consistent with the discussion in the section 3.2.

Using the expression (2.10), the mass of the soliton for both positive and negative energy bound states of the dynamical model as well as for the model with background soliton is shown in figure 6 with solid, dashed and dotted curves, respectively. The weak coupling approximation and the concept of the mass of the soliton based on the expression (2.10) is not valid at low θ_0 as can be seen in this graph, although for θ_0 greater than 1 these three curves coincide within the scale shown in the graph.

As a measure of the effect of the fermion on the soliton we calculate the root mean squared

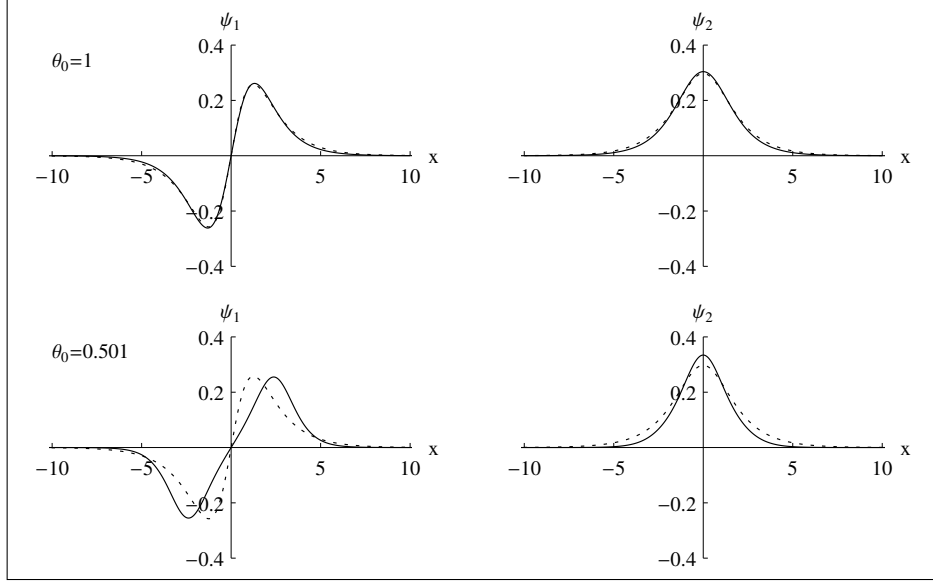


Figure 2. The positive energy fermionic bound state as a function of x for $\theta_0 = 1$ and $\theta_0 = 0.501$. Solid and dashed curves show the fermionic bound state in the dynamical model and in the weak coupling limit, respectively.

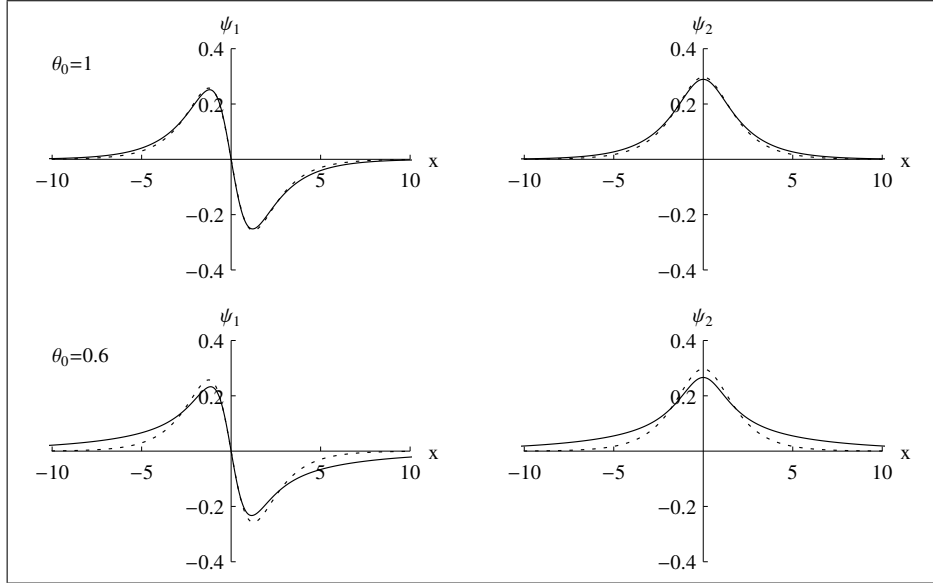


Figure 3. The negative energy fermionic bound state as a function of x for $\theta_0 = 1$ and $\theta_0 = 0.6$. Solid and dashed curves show the fermionic bound state in the dynamical model and the one in the weak coupling limit, respectively.

deviation between the static and dynamical soliton, δ_{RMS} . In figure 7, we show this result as a function of θ_0 and energy, for both positive and negative bound states. As expected, the back-reaction of the fermion on the soliton goes to zero when $E \rightarrow \pm\sqrt{3/2}$, i.e. the weak coupling limit. Interestingly, the right graph in this figure shows that the back-reaction decreases almost linearly with energy. Also, the left graph of this figure confirms that when θ_0 goes to zero the back-reaction

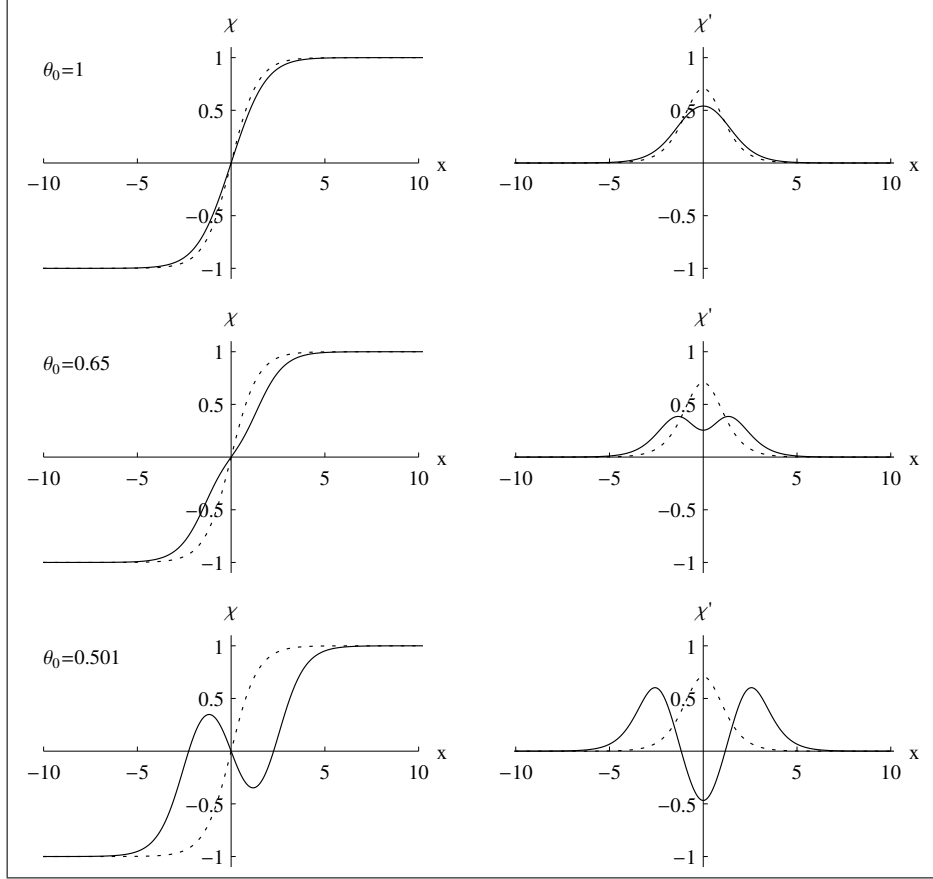


Figure 4. The bosonic field and its derivative with respect to x corresponding to positive bound energy for $\theta_0 = 1$, $\theta_0 = 0.65$ and $\theta_0 = 0.501$. Solid and dashed curves depict the bosonic field and its derivative in the dynamical model and the one in the weak coupling limit, respectively.

increases significantly and cannot be neglected in this region, i.e. the strong coupling region.

4 Conclusion

In this paper we investigate a minimal supersymmetric soliton model in two dimensions in which a static pseudo field is interacting nonlinearly with a Dirac particle. In this system the bosonic self interaction part of the potential that is responsible for creating a soliton with proper topological characteristics is considered to be the potential in $\lambda\phi^4$ theory. By varying the value of the bosonic field at spacial infinity, θ_0 , from zero to infinity we can span the whole region between the strong coupling limit and the weak coupling limit. In this system we find the zero mode fermionic state and threshold energies analytically, although in order to find other bound states and the corresponding shape of the soliton we need a numerical method. We use a relaxation method to calculate the energy spectrum and the bound states as well as the shape of the soliton. Our calculations show that despite the system not having particle conjugation symmetry except in the weak coupling limit, the back-reaction of the fermion on the soliton for the fermionic zero mode is zero. It means that although this symmetry is broken, it still has an imprint on the system. Therefore, the soliton corresponding to the fermionic zero mode is the known kink of $\lambda\phi^4$ theory for the whole interval of θ_0 . The analytic calculation of threshold states and the fact that they should match with bound

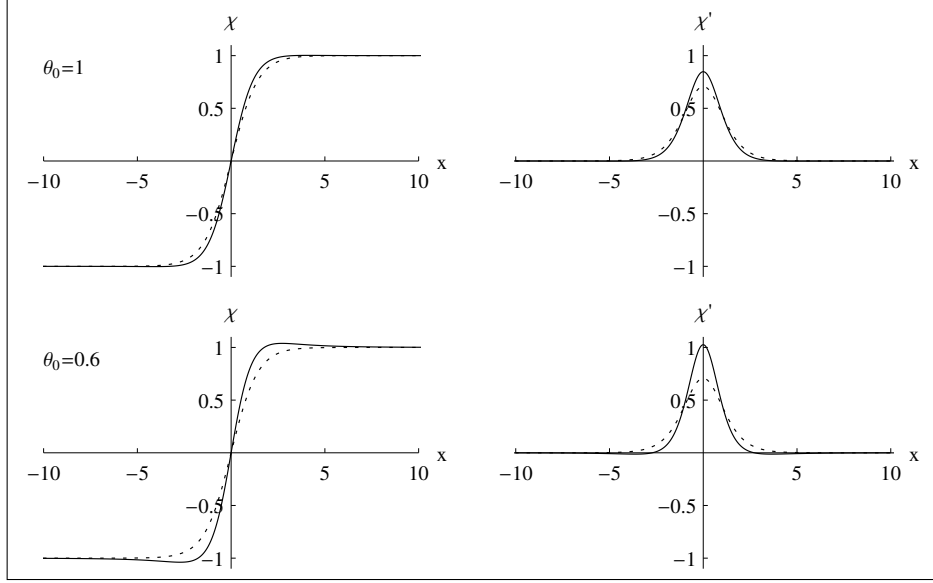


Figure 5. The bosonic field and its derivative with respect to x corresponding to negative energy for $\theta_0 = 1$ and $\theta_0 = 0.6$. Solid and dashed curves depict the bosonic field and its derivative in the dynamical model and the one in the weak coupling limit, respectively.

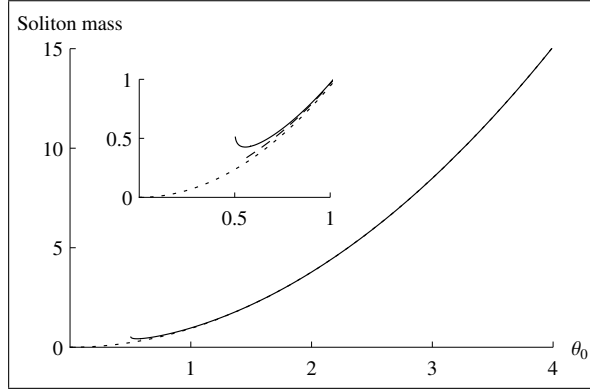


Figure 6. The soliton mass as a function of θ_0 . Solid and dashed curves show the soliton mass in the dynamical model corresponding to positive and negative energy, respectively. Dotted line is the soliton mass for the static model.

and continuum states out of the disturbance region show that except for the limit $\theta_0 \rightarrow 0$, no bound state joins to or arises from the continua besides the ones existing in the weak coupling limit. The shape of the soliton for positive and negative energy states that we calculate numerically also confirms this reasoning. We also calculate the so-called soliton mass and show that in the weak coupling region the dynamical and weak coupling approximation results coincide, though they are completely distinguishable in the strong coupling region. In the end, we calculate the back-reaction of the fermion on the soliton for the positive and negative energy states as a function of θ_0 and E . The results show that the back-reaction of the fermion on the soliton tends to zero as $\theta_0 \rightarrow \infty$ for both positive and negative bound energy curves, as expected. In contrast, when $\theta_0 \rightarrow 0$, the strong coupling limit, the back-reaction increases significantly which means that it cannot be omitted in

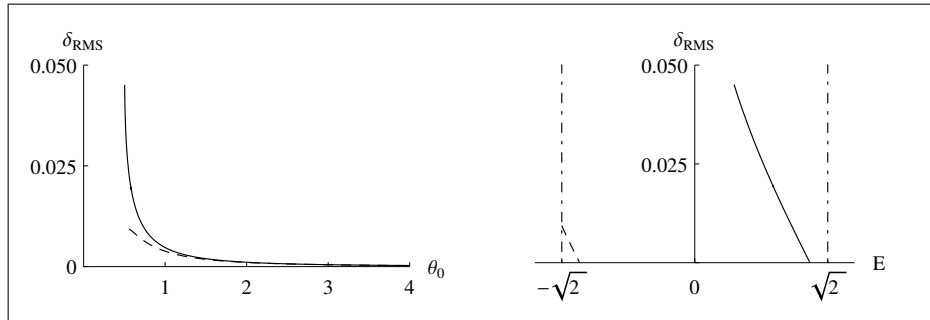


Figure 7. The back-reaction of the fermion on the soliton, δ_{RMS} , as a function of θ_0 and the fermionic bound energy E . Solid and dashed curves show the back-reaction corresponding to the positive and negative energy, respectively, in the dynamical model. Dotdashed lines are the threshold energies in the weak coupling limit.

the strong coupling region.

Acknowledgments

A. Mohammadi and A. Amado thank Conselho Nacional de Desenvolvimento Científico e Tecnológico (CNPq) for financial support.

References

- [1] N. J. Zabusky and M. D. Kruskal, Phys. Rev. Lett. **15**, 240 (1965).
- [2] D. J. Korteweg and F. de Vries, Philos. Mag. **39**, 422 (1895).
- [3] R. Rajaraman, *Solitons and Instantons* (North-Holland, Amsterdam,1982).
- [4] P. Drazin and R. Johnson, *Solitons: an Introduction* (Cambridge University Press, Cambridge,1996).
- [5] N. Manton and P. Sturcliffe, *Topological Solitons* (Cambridge University Press, Cambridge,2004).
- [6] H. Watanabe and H. Murayama, Phys. Rev. Lett. **112**, 191804 (2014).
- [7] R. Driben, Y. V. Kartashov, B. A. Malomed, T. Meier and L. Torner, Phys. Rev. Lett. **112**, 020404 (2014).
- [8] K. V. Samokhin, Phys. Rev. **B 89**, 094503 (2014).
- [9] E. R. Bezerra de Mello and A. A. Saharian, JHEP **04**, 046 (2009).
- [10] A. I. Milstein, I. S. Terekho, U. D. Jentschura and C. H. Keitel, Phys. Rev. **A 72**, 052104 (2005).
- [11] T.H.R. Skyrme, Proc. Roy. Soc. London **A 247**, 260 (1958).
- [12] T.H.R. Skyrme, Proc. Roy. Soc. London **A 252**, 236 (1959).
- [13] T.H.R. Skyrme, Proc. Roy. Soc. London **A 260**, 127 (1961).
- [14] T.H.R. Skyrme, Nucl. Phys. **31**, 556 (1962).
- [15] T.H.R. Skyrme, J. Math. Phys. **12**, 1735 (1971).
- [16] W.A. Bardeen, M.S. Chanowitz, S.D. Drell, M. Weinstein and T.-M. Yan, Heavy quarks and strong binding: a old theory of hadron structure, Phys. Rev. **D 11**, 1094 (1975).
- [17] R. Friedberg and T.D. Lee, Fermion old nontopological solitons. 1, Phys. Rev. **D 15**, 1694 (1977).

- [18] R. Friedberg and T.D. Lee, Fermion eld nontopological solitons. 2. Models for hadrons, Phys. Rev. **D 16**, 1096 (1977).
- [19] R. Jackiw and C. Rebbi, Phys. Rev. **D 13**, 3398 (1976).
- [20] F. Charmchi and S. S. Gousheh, Nucl. Phys. **B 883**, 256 (2014).
- [21] E. R. Bezerra de Mello and A. A. Saharian, Eur. Phys. J. C **73**, 2532 (2013).
- [22] S.S. Gousheh, A. Mohammadi and L. Shahkarami, Phys. Rev. **D 87**, 045017 (2013).
- [23] L. Shahkarami, A. Mohammadi and S.S. Gousheh, JHEP **11**, 140 (2011).
- [24] R. F. Dashen, B. Hasslacher and A. Neveu, Phys. Rev. **D 10**, 4130 (1974).
- [25] A. K. Kaul and R. Rajaraman, Phys. Lett. **B 131**, 357 (1983).
- [26] A. Rebhan, P. van Nieuwenhuizen and R. Wimmer, Braz. J. Phys. **34**, 1273 (2004).
- [27] M. A. Shifman and A. I. Vainshtein and M. B. Voloshin, Phys. Rev. **D 59**, 045016 (1999).
- [28] H. Nastase, M. Stephanov, P. van Nieuwenhuizen and A. Rebhan, Nucl. Phys. **B 542**, 471 (1999).
- [29] N. Graham and R. L. Jaffe, Nucl. Phys. **B 544**, 432 (1999).
- [30] L. Alvarez-Gaume, S. F. Hassan, Fortsch, Phys. **45**, 159 (1997).
- [31] N. Seiberg and E. Witten, Nucl. Phys. **B 426**, 19 (1994); Nucl. Phys. **B 431**, 484 (1994).
- [32] F. Charmchi and S. S. Gousheh, Phys. Rev. **D 89**, 025002 (2014).
- [33] L. Shahkarami and S.S. Gousheh, JHEP **06**, 116 (2011).
- [34] Shi-Hai Dong, Xi-Wen Hou and Zhong-Qi Ma, Phys. Rev. **A 59**, 995 (1999).
- [35] Shi-Hai Dong, Xi-Wen Hou and Zhong-Qi Ma, Phys. Rev. **A 58**, 2160 (1998).